Time-Resolved Visible and Infrared Study of the Cyano Complexes of Myoglobin and of Hemoglobin I from *Lucina pectinata*

Jan Helbing,* Luigi Bonacina,† Ruth Pietri,‡ Jens Bredenbeck,* Peter Hamm,* Frank van Mourik,† Frédéric Chaussard,† Alejandro Gonzalez-Gonzalez,† Majed Chergui,† Cacimar Ramos-Alvarez,‡ Carlos Ruiz,‡ and Juan López-Garriga‡

*Physikalisch-Chemisches Institut, Universität Zürich, Zürich, Switzerland; †Laboratoire de Spectroscopie Ultrarapide, Institut des Sciences et Ingénierie Chimiques, Faculté des Sciences de Base, Ecole Polytechnique Fédérale de Lausanne, Lausanne-Dorigny, Switzerland; and ‡Chemistry Department, University of Puerto Rico, Mayagüez, Puerto Rico

ABSTRACT The dynamics of the ferric CN complexes of the heme proteins Myoglobin and Hemoglobin I from the clam *Lucina pectinata* upon Soret band excitation is monitored using infrared and broad band visible pump-probe spectroscopy. The transient response in the UV-vis spectral region does not depend on the heme pocket environment and is very similar to that known for ferrous proteins. The main feature is an instantaneous, broad, short-lived absorption signal that develops into a narrower red-shifted Soret band. Significant transient absorption is also observed in the 360–390 nm range. At all probe wavelengths the signal decays to zero with a longest time constant of 3.6 ps. The infrared data on MbCN reveal a bleaching of the C ≡ N stretch vibration of the heme-bound ligand, and the formation of a five-times weaker transient absorption band, 28 cm^{-1} lower in energy, within the time resolution of the experiment. The MbC ≡ N stretch vibration provides a direct measure for the return of population to the ligated electronic (and vibrational) ground state with a 3–4 ps time constant. In addition, the CN-stretch frequency is sensitive to the excitation of low frequency heme modes, and yields independent information about vibrational cooling, which occurs on the same timescale.

INTRODUCTION

Heme proteins are widely studied as model systems to understand structure-function relationships and ligand-binding properties. Invertebrate hemoglobins are especially interesting because of their functional ability to bind molecules other than O_2 (Terwilliger, 1998). *Lucina pectinata*, for instance, is a clam which contains a unique hemoglobin (HbI) that is involved in H_2S transport. For its food supply this mollusk incorporates a vast population of chemoautotrophic symbiotic bacteria, which must be supplied with the environmental H_2S found in the sediments in which the clam lives. The monomeric HbI, located in the symbiont-harboring gills of *L. pectinata*, reacts with H_2S with an extraordinary affinity (Kraus and Wittenberg, 1990; Wittenberg and Kraus, 1991), and delivers the ligand to the bacteria. However, in contrast to more common ligands like O_2, NO, or CO, which bind to ferrous heme proteins (Fe^{II}), hydrogen sulphide binds to Hemoglobin I in its ferric state (Fe^{III}). The x-ray crystal structure of the aquomet complex has revealed that HbI is structurally very similar to vertebrate Myoglobin. However, a glutamine residue instead of the typical histidine occupies the distal position 64, and there is an unusual distribution of aromatic residues (Phe-29, Phe-68, and Phe-28), surrounding the heme distal position (Rizzi et al., 1994).

The present study of hemoglobin I and myoglobin was initiated to gain better insight into the interaction between the ligand and the heme pocket, by comparing the ultrafast dynamics of ligand dissociation and rebinding in the two proteins. It has been proposed that the extent of geminate ligand recombination after photolysis is sensitive to the interaction of a ligand with the distal amino acid residues and the possibility of that ligand being trapped within the heme pocket (Martin and Vos, 1994; Kholodenko et al., 1999a). Since H_2S is an unsuitable ligand for a comparative study, as it only binds to HbI from *L. pectinata* (Kraus and Wittenberg, 1990), we chose the cyanide anion CN^- as ligand, which forms low-spin ferric complexes both with HbI and vertebrate heme proteins (Cerda et al., 1999).

Ligand dynamics upon femtosecond laser excitation of hemoglobins and myoglobins has been intensely studied for almost two decades (Martin and Vos, 1994; Petrich et al., 1987, 1988; Lim et al., 1995a, 1996; Kholodenko et al., 1999b; Franzen et al., 2001; Ye et al., 2002) but, owing to their relevance in the respiratory system of vertebrates, most attention has been paid to globins with the iron atom in the ferrous state. Indeed, although there exists a large amount of information from a variety of experimental studies on the ground-state properties of heme proteins in the ferric state, and in particular the CN complex (Yoshikawa et al., 1985; Boffi et al., 1997; Schweitzer-Stenner et al., 2000; Das et al., 2000), little is known about its ultrafast dynamics after laser excitation. On a femtosecond timescale, cyano complexes have only been investigated in an early study on cooperative effects in the binding properties of human hemoglobin (Petrich et al., 1988). In that study complete ground-state recovery within a few picoseconds after laser excitation was

Submitted October 24, 2003, and accepted for publication June 14, 2004.

Address reprint requests to Jan Helbing, Dept. of Physical Chemistry, University of Zürich, Winterthurerstrasse 190, 8057 Zürich, Switzerland. Tel.: 41-1-635-4471; E-mail: j.helbing@pci.unizh.ch.

0006-3495/04/09/1881/11 $2.00

doi: 10.1529/biophysj.103.036236

observed, but no analysis of possible reaction mechanisms was carried out. More recently, dissociation of NO from ferric myoglobin was reported (Cao et al., 2001), which led to the formation of met-myoglobin (a five-coordinate, high-spin heme with a water molecule inside the heme pocket, Vojtechovsky et al., 1999) on a millisecond timescale. Two fast time constants in the dynamics (0.7 and 4.6 ps) were attributed to electronic relaxation and cooling of heme (Cao et al., 2001). The scarcity of detailed investigations of ferric complexes with high time resolution is especially surprising, as charge transfer processes that involve the central metal atom are commonly invoked to account for ligand photolysis and electronic relaxation of photoexcited metal porphyrins (Steiger et al., 2000; Franzen et al., 2001). These should be very sensitive to the oxidation state of the complex under investigation, which calls for a systematic study of the photodynamics of a heme protein with a ferric ground state.

To this aim, we carried out femtosecond pump-probe transient absorption measurements in the 360–600 nm region after Soret band excitation of the HbICN and MbCN complexes, with largely different heme pocket environments. The data reveal identical ultrafast kinetics in both proteins with a spectral evolution very similar to that typical for ferrous heme proteins. In addition, transient mid-infrared absorption measurements have been performed that directly monitor the dynamics of the CN ligand to myoglobin. The infrared data provides direct information on the recovery of the ligated electronic ground state as well as vibrational cooling, and allow a detailed analysis of the ultrafast dynamics of a ferric heme complex.

EXPERIMENTAL

Samples

Met-myoglobin from horse skeletal muscle (molecular weight ~18,000) was purchased from Sigma-Aldrich (St. Louis, MO) and used without further purification. For optical measurements, the protein was dissolved in 0.1 M phosphate buffer solution (pH 7) to a concentration of ~100 μM. For infrared (IR) measurements 10–18 mM solutions were prepared in deuterated phosphate buffer (pD 7). In both cases, the CN complex was formed by adding 2–3-fold excess of potassium cyanide (either $^{12}C^{14}N$ or the $^{13}C^{15}N$ isotope). *L. pectinata* was collected from the shallow mangroves near La Parguera, Puerto Rico. Isolation and purification of HbI from the clam was achieved according to methods described previously (Wittenberg and Kraus, 1991; Petrich et al., 1988). In brief, oxyHbI was isolated by gel filtration chromatography on a Sephadex G-75 column (Pharmacia, Uppsala, Sweden) equilibrated with a 50 mM phosphate buffer solution, pH 7.5, containing 0.5 mM EDTA. OxyHbI was further purified by ion exchange chromatography on a DEAE Sephadex A-50 column (Pharmacia) equilibrated with 25 mM ammonium bicarbonate buffer, pH 8.3. The HbI-CN complex was prepared by oxidation of oxyHbI with a 10% excess of potassium ferricyanide to obtain ferric HbI and then by adding a slight excess of potassium cyanide. Complex formation was verified periodically by monitoring the UV-visible (UV-vis) spectrum, which exhibits a characteristic Soret band at 421 nm (HbICN) or 422 nm (MbCN), and a broad visible band at 540 nm (Q-band). UV-vis absorption spectra were also recorded before and after laser measurements to check for sample integrity.

Cells

For the UV-visible measurements the MbCN solution was flown in a closed cycle through a quartz flow cell with 500-μm optical path length. The optical density at the maximum of the Soret band was typically ~0.6 optical density (OD). A sealed, 1-mm-pathlength spinning sample cell made of 2-mm CaF_2 windows was used for HbI (OD = 1.2−1.6). IR measurements were carried out in a flow cell, consisting of two 2-mm-thick CaF_2 windows held apart by 50-μm or 100-μm Teflon spacers, and protein solution was circulated by a peristaltic pump in a closed circuit especially designed to handle small sample volumes (Bredenbeck and Hamm, 2003).

Laser measurements

Femtosecond (fs) pulses were generated by amplified titanium-sapphire laser systems (Spectra Physics, Mountain View, CA), that produce 700-μJ pulses near 800 nm at a repetition rate of 1 kHz. Pump pulses centered at 405 nm (optical measurements) or 420 nm (IR measurements) were obtained by second harmonic generation in a 500-μm β-barium-borate crystal. The pump pulses were passed through an optical delay line and a chopper which cut out every second pulse. Whereas short (~100 fs) pulses with relatively low energy (~1 μJ) were used in the optical measurements, the 420-nm pulses used in the IR setup were stretched to 600–700 fs duration by guiding them through 25 cm of fused silica. This significantly increased the threshold for undesired nonlinear effects in the sample such as white-light generation and/or color center formation and allowed excitation of a large fraction of the molecules in the sample (~20%). Probe pulses for optical measurements were produced by focusing a small portion of 800-nm light into a 20-mm-thick CaF_2 window to generate a white-light continuum with a low wavelength cutoff near 390 nm. Measurements in the 360–400-nm region were carried out with white light produced from frequency-doubled 400-nm laser pulses. The white light was focused onto the sample using all-reflective optics, and the chirp inside the sample cell was determined by measuring the laser-induced Kerr signal of the solvent. In the 420–600-nm region it was typically of the order of 1.3 fs/nm and close to linear. Infrared probe pulses near 2000 cm^{-1} (100 fs, 1 μJ, 300 cm^{-1} bandwidth) were produced by a homebuilt double-stage optical parametric amplifier followed by frequency mixing in a $AgGaS_2$ (silver thiogallate) crystal (Hamm et al., 2000). Both in the visible and the infrared experiments, the probe pulses were split into two parts. One part (the probe pulse) was overlapped with the pump pulse in the sample cell. The second part was used as a reference beam to correct for intensity fluctuations. Both beams were focused onto the entrance slit of a monochromator where they were dispersed, and spectra were detected either with a double-photodiode array (2 × 256 pixels, 1-nm resolution) or a double MCT array (2 × 32 pixels, 2-cm^{-1} resolution) on a single-shot basis.

RESULTS

UV-vis data

Transient spectra in the Soret and Q-band region of MbCN at different delays after excitation with a 400-nm pump pulse can be seen in Fig. 1. For comparison, the inset shows the corresponding spectra recorded for the HbICN complex, which were found to be almost identical. In particular, the signals for both proteins completely decay to zero with the same time constant. Next to the bleach of the Soret band there is an immediate increase in absorption in the 450–500-nm region with a maximum near 480 nm. After only 500 fs this broad feature has almost disappeared again, and the transient spectrum now shows a peak near 440 nm. As this absorption feature grows in, it continuously shifts to shorter

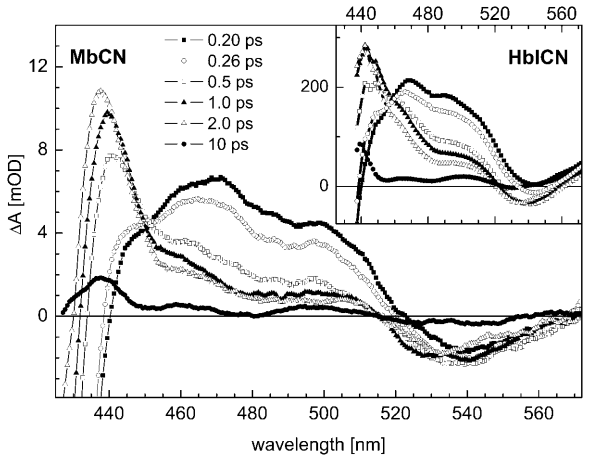

FIGURE 1 Transient absorption signals for probe delays 200 fs, 260 fs, 500 fs, 1 ps, 2 ps, and 10 ps after excitation of MbCN by a 80-fs pump pulse at 400 nm. The inset shows the same data for the HbICN complex from *L. pectinata*.

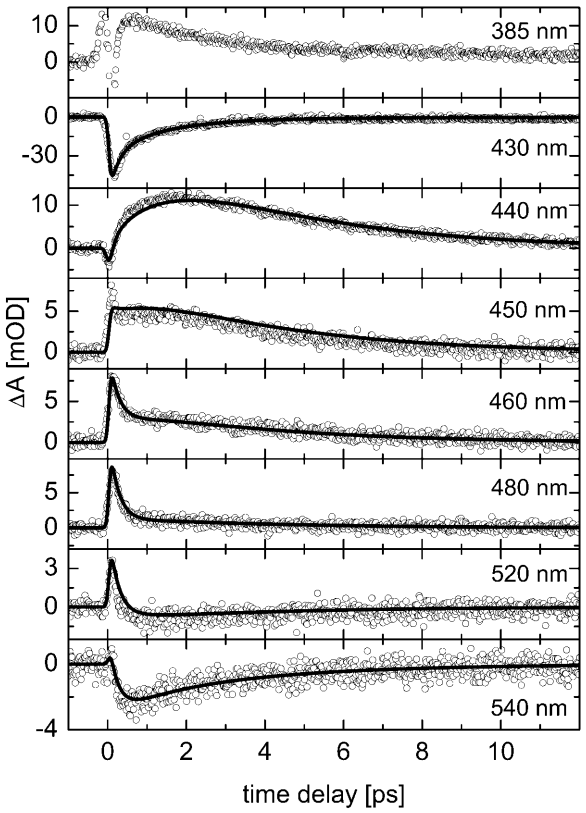

FIGURE 2 Transient absorption changes at different probe wavelengths. The solid lines show the result of a global fit with three time constants 230 fs, 1.3 ps, and 3.6 ps. Note the different vertical scales.

wavelengths. At the same time there is a steady decrease in the amplitude of the Soret bleach. The spectra also reveal a blue shift of the local absorption minimum near 540 nm, which is due to the bleaching of the Q-band. Transients at selected probe wavelengths for MbCN are shown in Fig. 2. Positive absorption near 440 nm is largest at a pump-probe delay of 2 ps. At longer delays the transient absorption signal decays on a 4-ps timescale at all wavelengths. This later phase in the dynamics is characterized by an isosbestic point near 430 nm, reflecting the fact that only minor spectral shifts take place in the Soret region after ~4 ps (*second trace* in Fig. 2). A transient increase in absorption is also observed to the blue side of the Soret bleach, with a maximum in the transient spectra near 385 nm. At this wavelength the signal is largest at a pump-probe delay of 800 fs, and reaches almost the same maximal amplitude as the signal at 440 nm. It then decays on a 1.5–4-ps timescale.

For better comparison with previous work on ferrous systems, we have performed a global fit by applying singular value decomposition to the chirp-corrected data and analyzing the basis time traces which correspond to the first largest singular values. These were simultaneously fitted by a linear combination of three exponentials convoluted with a Gaussian function to take into account the finite time resolution. The solid lines in Fig. 2 show the result of this fit, which yields time constants of 230 fs, 1.3 ps, and 3.6 ps. Significantly poorer agreement was found when fitting with only two time constants. The spectra $S_{\tau k}$ associated with each of the three time constants are shown in Fig. 3. The time constants and their wavelength-dependent weight compare well with results obtained for ferrous heme proteins (Franzen et al., 2001), which suggests that the underlying dynamics is very similar for the ferric systems studied here. Note, however, that decay-associated spectra only yield physical insight into the dynamics, if the transient spectra consist of state- or species-associated bands which only change in intensity. An absorption band that also changes its shape or spectral position as a function of time is only poorly captured by this analysis. It has recently been shown that the transient absorption signal of deoxy myoglobin can be well-reproduced by superposition of the ground-state absorption spectrum and a single broadened and red-shifted Soret band which narrows and shifts back to equilibrium with time-constants of 400 fs and 4 ps, respectively (Ye et al., 2003). Indeed, already a very simple simulation for MbCN with similar parameters allows us to qualitatively capture the main features in our experimental data. Unfortunately, this analysis could not be carried out in full detail here, since different spectral components make up the absorption spectrum of MbCN in the Soret region (Schweitzer-Stenner et al., 2000), and their different broadening behavior is not known.

Infrared measurements

The Fourier-transform infrared (FTIR) absorption spectrum of MbCN in deuterated phosphate buffer at pD 7 between 2000 and 2200 cm^{-1} consists of a single narrow peak at 2126 cm^{-1}, with a width of 9–10 cm^{-1} (*top left* in Fig. 4). Since the pK value of HCN is 9.3, the excess cyanide that is not

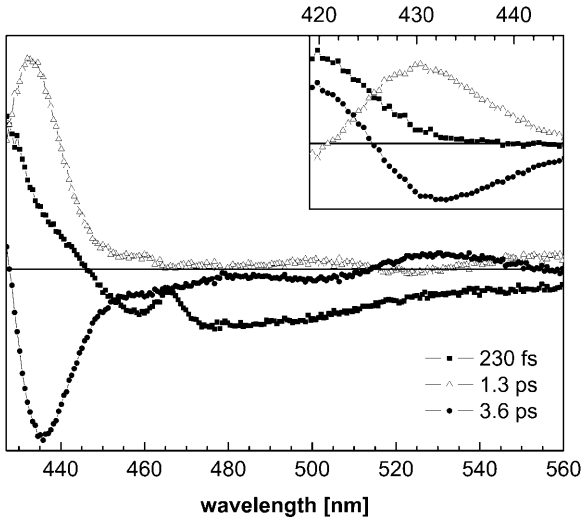

FIGURE 3 Spectral components $S_{\tau k}$ associated with the three time constants 230 fs (*squares*), 1.3 ps (*open triangles*), and 3.6 ps (*circles*), required to fit the transient spectra of MbCN. The dip in the 230-fs spectrum near 465 nm is due to the coherent Raman signal of the H_2O solvent. The inset shows an enlarged view of the Soret band region (data from a more dilute sample).

bound to the protein is almost entirely deuterated in the D_2O buffer, and no CN^- absorption band is seen at 2079 cm^{-1}. The DC ≡ N stretch vibration is observed at 1887 cm^{-1} in deuterated buffer solutions (Yoshikawa et al., 1985), much lower in energy than the HC ≡ N stretch (absorption at 2093 cm^{-1}, ϵ = 30 L M^{-1} cm^{-1}). The use of isotope-labeled $^{13}C^{15}N$ lowers the MbC ≡ N stretch frequency by 77 cm^{-1} to 2049 cm^{-1}, almost exactly as expected from a reduced mass calculation for CN (2048 cm^{-1}), without significantly changing bandwidth or intensity (*top right* in Fig. 4). We used the visible absorption of our samples (ϵ =11,300 L M^{-1} cm^{-1} at 540 nm) to determine the protein concentration, and obtain an extinction coefficient for the 2126 cm^{-1} band of 100 ± 20 L M^{-1} cm^{-1}. This is comparable to the value reported in Yoshikawa et al. (1985, 70 L M^{-1} cm^{-1}) but much smaller than reported in Reddy et al. (1996, 250 L mM^{-1} cm^{-1}). As a consequence of this small extinction coefficient, the transient IR measurements had to be carried out with an infrared absorbance of only 5–10 mOD.

Upon UV excitation of the Soret band of CN-ligated myoglobin, the transient infrared spectra show a strong bleach of the MbC ≡ N stretch fundamental near 2126 cm^{-1}, as well as two smaller absorption features, one immediately to the red of the bleach, and one red-shifted by ~30 cm^{-1}. These are labeled *1* and *2* in Fig. 4, respectively. Band 2, initially centered at 2093 cm^{-1}, is approximately five-times weaker than the bleaching signal at 2126 cm^{-1}. It decays with increasing pump-probe delay and its maximum shifts toward larger energies (see also Fig. 5). A similar blue shift can also be seen for the minimum of the bleaching signal, which weakens at the same rate as band 2.

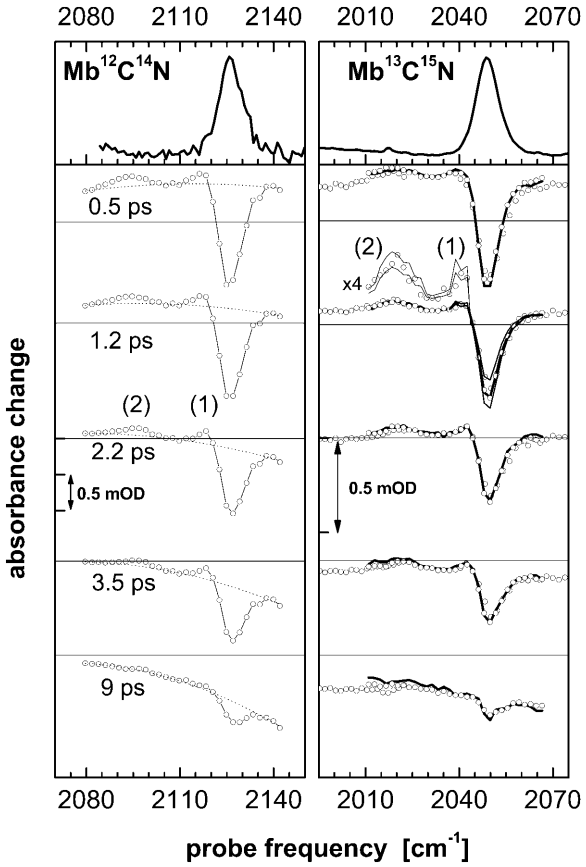

FIGURE 4 (*Top*) FTIR absorption spectra of $Mb^{12}C^{14}N$ (*left*) and $Mb^{13}C^{15}N$ (*right*) in deuterated phosphate buffer at pD 7. (*Bottom*) Corresponding transient absorption signals at different probe delays after excitation of MbCN by a 700-fs pump pulse at 420 nm. The dotted lines show a quadratic fit to the background signal, caused mainly by the rise in solvent temperature. The signals for parallel polarization of pump and probe pulses ($Mb^{13}C^{15}N$, *lines*) were multiplied by a factor $R = 1.5$ to superimpose them on the signals for perpendicular polarization (*open circles*). The lines in the enlarged view (4×) show the parallel signal multiplied by $R = 1.2$ ($\alpha \approx 40°$) and by $R = 1.7$ ($\alpha \approx 20°$).

The transient absorption signals of MbCN are superimposed on a broad background signal, which is initially positive and caused by cross-phase modulation between overlapping pump and probe pulses in the D_2O solvent as well as the CaF_2 windows of the flow cell. At longer pump-probe delays, the background signal becomes negative and tilted toward larger frequencies. It is well-known that the infrared absorption bands of liquid water shift toward higher energies with increasing temperatures, giving rise to a negative pump-probe signal at the low energy side of the D_2O stretch vibration. This has been attributed to a weakening of hydrogen bonding, which results in the strengthening of the intramolecular bonds. The time dependence of the background signal thus provides a measure for the transfer of (thermal) energy, originally localized on the porphyrin chromophore, to the solvent. It takes place on a 5–10-ps

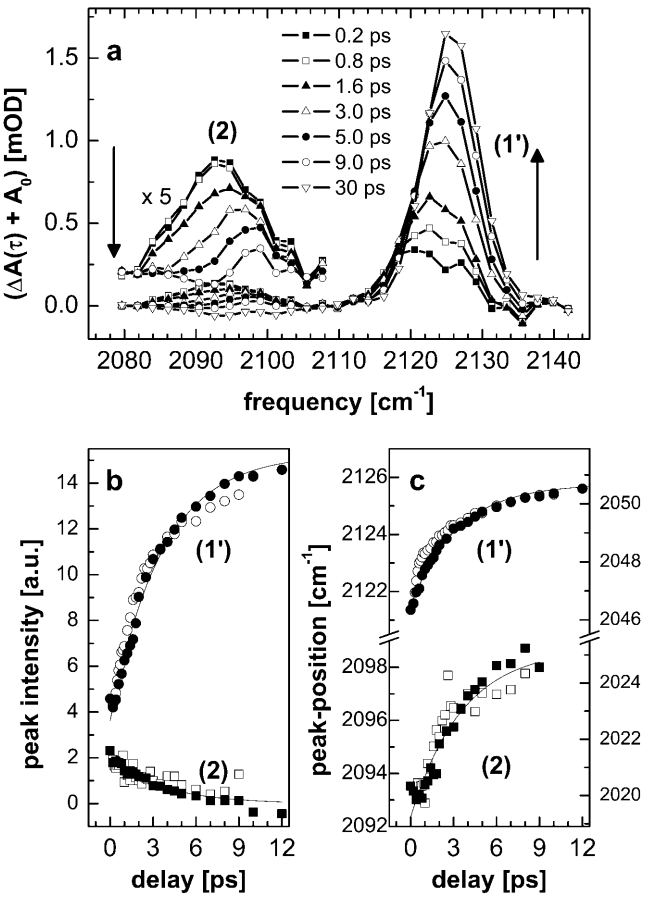

FIGURE 5 (*a*) Transient absorption signals of $Mb^{12}C^{14}N$, with the bleaching component eliminated by adding the same scaled FTIR absorption spectrum A_0, and subtracting the second-order polynomial fit to the background (*dotted lines* in Fig. 4) from all spectra. The intensities and peak positions of the bands labeled *1* and *2* were determined by fitting Gaussian lineshapes and are shown in *b* and *c*, respectively. The solid lines are exponentials with a fixed 3.6-ps time constant.

timescale, which is very similar to what has been previously reported for closely related systems (Lian et al., 1994).

To reduce this background signal, experiments were also carried out using the $^{13}C^{15}N$ isotope as ligand (*right-hand side* of Fig. 4). Apart from the shift in CN-stretch frequency, almost identical results were obtained. The small product band at 2020 cm^{-1} is equally red-shifted by 28 cm^{-1} with respect to the fundamental MbC ≡ N stretch transition, and is of the same relative strength with respect to the MbCN bleach. No other bands were observed in the 1970–2100-cm^{-1} spectral range.

Transient spectra are difference spectra and can be viewed as the superposition of a negative bleaching component, which is time-independent and has the shape of the absorption spectrum before excitation, and the time-dependent positive absorption of those molecules that have been excited by the pump pulse. For a better visualization of the temporal evolution it is instructive to eliminate the bleaching component from the transient spectra by adding the FTIR absorption spectrum with the same scaling factor for all time delays. (The scaling factor was determined by fitting the FTIR spectrum to the 0.5-ps signal in the 2130–2145 (2050–2065) cm^{-1} spectral range (blue wing) of the main bleach. This yields the smallest possible value that eliminates negative contributions from the signal after background subtraction. The ground-state population derived from Fig. 5 is therefore associated with relatively large error bars and may be underestimated.) The resulting pump-probe spectra contain only positive signals, which reflect the time-dependent absorption of those molecules that have absorbed a UV photon (Fig. 5 *a*). The return of excited molecules to the (electronic and/or vibrational) ground state now appears as a growth of the fundamental MbC ≡ N stretch absorption band. It can be seen that at early time delays this band (labeled 1′) does not appear at 2126 cm^{-1}, but is shifted to smaller energies, with a considerably larger width. It is this shift and broadening of the MbC ≡ N stretch transition that leads to the positive signal *1* in the transient spectra of Fig. 4. The time-dependent intensities (area) and central frequencies of the two bands in Fig. 5 *a* were extracted by least-square fitting with Gaussian lineshapes, and are shown as a function of pump-probe delay in Fig. 5, *b* and *c*. The decay of band 2 and the recovery of the fundamental MbC ≡ N stretch absorption occur exactly in parallel and can be well reproduced by an exponential function with the 3.6-ps time constant obtained from the fit of the visible data (*solid lines* in Fig. 5 *b*). Very similar exponential dynamics are found for the position of the corresponding band maxima (Fig. 5 *c*). Both undergo a blue-shift of ~4 cm^{-1} on the same 3–4-ps timescale.

Finally, the signal anisotropy was determined from the quasisimultaneous measurement of the transient absorption changes with parallel and perpendicularly polarized pump and probe laser pulses. At all pump-probe delays the same scaling factor of 1.5 ± 0.2 is needed to completely overlap the spectra recorded with parallel and perpendicular polarizations (*solid lines* in Fig. 4). The anisotropy is thus identical for all bands in the transient absorption spectra, and does not change with time. For a plane-polarized pump transition (the Soret transition is doubly degenerate) and a linearly polarized probe transition, the angle α between the C ≡ N axis and the normal to the heme plane is related to the polarization ratio via (Moore et al., 1988)

$$R = \frac{\Delta A_{\perp}}{\Delta A_{\parallel}} = \frac{4 - \sin^2 \alpha}{2 + 2\sin^2 \alpha}. \quad (1)$$

The observed value of $R = 1.5 \pm 0.2$ corresponds to an angle of 30 ± 8°. This value (which is an upper limit since possible saturation of the transition and imperfect polarizers tend to lower the observed anisotropy) can be compared with results of NMR studies, which measured a ≈15° tilt of the Fe-C ≡ N unit with respect to the heme normal (Rajaratham

et al., 1992) and polarized infrared absorption measurements on Mb single crystals, which yielded a tilt of 21–22° (Sage, 1997).

DISCUSSION

In the following we first assign the transient mid-infrared absorption bands, and show that they provide information on both vibrational cooling and relaxation of electronic excitation of the heme. We then discuss the optical response in the Soret and Q-band region in direct comparison with previous studies of ferrous heme proteins.

Assignment of the transient infrared absorption bands

Two positive absorption features are present in the transient infrared spectra in the 2000–2200-cm^{-1} region. The band labeled *1* in Fig. 4, immediately next to the bleaching signal of the equilibrium MbC ≡ N stretch fundamental, is a typical signature of an increased vibrational temperature in the molecule, which shifts the C ≡ N transition to lower frequencies. This frequency shift can be understood as the result of thermal (or nonthermal) excitation of low frequency modes of the heme (or protein), which anharmonically couple to the C ≡ N stretch vibration (Hamm et al., 1997b). The small red-shift associated with band *1* can therefore be viewed as an indicator of the temperature of CN-ligated molecules in the electronic ground state. This is better seen in Fig. 5, where the bleaching signal of equilibrium MbCN species has been subtracted. From the intensity of band *1′* in this figure, we can directly read off the fraction of molecules which have returned to the CN-ligated electronic ground state (*trace 1′* in Fig. 5 *b*). It appears that within the time resolution of our experiment at least 25% of the initially excited molecules are CN-bound and electronically relaxed, but vibrationally hot. The full return of the signal to the equilibrium spectrum then takes place with a 3–4-ps time constant and involves both population relaxation, as reflected by the changes in signal intensity, and heme cooling, i.e., the de-excitation of the anharmonically coupled low-frequency modes that are responsible for the observed frequency shift of the CN stretch vibration. The timescale of vibrational cooling of heme in MbCN is thus very similar to the 3 ± 1 ps deduced from time-resolved anti-Stokes Raman measurements upon photolysis of MbCO (Mizutani and Kitagawa, 1997).

Information about the nature of population relaxation is provided by the second transient absorption band (labeled *2* in Fig. 4). It appears ~30 cm^{-1} to the red of the equilibrium MbC ≡ N stretch fundamental, very close to the spectral position of the HC ≡ N vibration in aqueous solution. Since the absorbance of the C ≡ N stretch band of free CN^-, HCN, or DCN is also 3–5-times weaker than that of heme-bound CN (Reddy et al., 1996), spectral position and low intensity of band 2 may suggest that it arises from ligand dissociation. However, two observations speak against the assignment of band 2 to fully photodissociated CN^- ligands:

1. The signal anisotropy, which is constant in time and identical for product bands and bleach, shows that the CN angle relative to the heme plane does not change significantly. (Signal/noise at delays <4 ps is high enough to exclude differences in angle of >20°.)
2. The time-dependent frequency shift of band 2 implies coupling to the thermally excited low-frequency modes of the heme, which is very similar to the coupling responsible for the spectral shifts of band 1′.

Thus, CN associated with band 2 cannot be moving freely inside the heme pocket and must still be in close contact with the macrocycle. This leaves two possible assignments, which are discussed separately: Band 2 could either represent the C ≡ N stretch fundamental in a more loosely bound, electronically excited state, or it could be due to the $v = 1 \rightarrow v = 2$ transition of heme-bound ligands that have become vibrationally excited in the photoprocess.

Vibrational excitation of the C ≡ N stretch

The possibility that band 2 is a result of the excitation of one quantum of C ≡ N stretch is suggested by the observation that the 28-cm^{-1} frequency shift with respect to the bleaching signal is very similar to the anharmonicity of the CN^- stretch vibration in water (the $v = 1 \rightarrow v = 2$ transition of $^{13}C^{15}N^-$ in D_2O is 26-cm^{-1} lower in energy than the $v = 0 \rightarrow v = 1$ fundamental; Hamm et al., 1997a). In addition, this assignment would nicely explain why the maxima of bands 1 and 2 in Fig. 5 blue-shift by nearly the same amount and in parallel during heme-cooling. However, in the case of vibronic excitation, the negative signal from the $0 \rightarrow 1$ transition (bleach and stimulated emission) should have the same intensity as the $1 \rightarrow 2$ absorption band. In contrast, band 2 is approximately five-times weaker than the bleaching signal, and this intensity ratio is maintained at all time delays. As a result, the molecules with one quantum of excitation in the C ≡ N stretch can only represent a small fraction of the excited species (excitation to higher vibrational levels was not observed). The main fraction of excited molecules would have to be invisible in the mid-infrared spectrum before they return to the CN-ligated electronic ground state on a 3–4 ps timescale. In Fig. 6 *a* we show a relatively simple kinetic scheme that would be able to account for these observations. Before becoming observable again in the 2000–2200-cm^{-1} region of the mid-infrared spectrum, excited molecules could populate a state $|e\rangle$, characterized either by a very broad and/or strongly frequency-shifted distribution of C ≡ N stretch frequencies with a very weak extinction coefficient. The decay of state $|e\rangle$ would lead to population of the CN-ligated electronic ground state with rate constants constrained by the observation that decay of band 2 (i.e., the $v = 1$ vibrationally excited state in this scheme) and the recovery of the MbC ≡ N

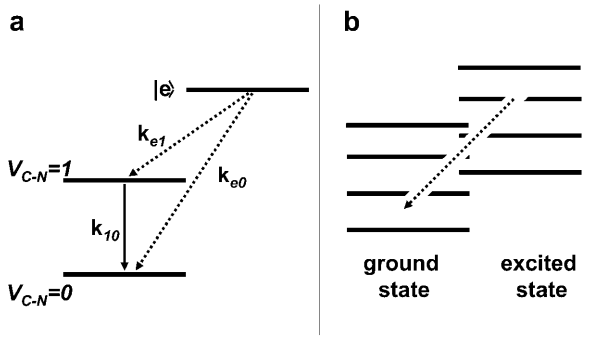

FIGURE 6 Two alternative kinetic models to account for the transient absorption changes in the C ≡ N stretch region. (*a*) The lower two levels represent MbCN in the electronic ground state with no or one quantum of excitation in the CN stretch mode. They are populated by the decay of an excited or unligated state |e⟩ with no detectable infrared absorption in the spectral region investigated. (*b*) The red-shifted IR band 2 is due to a more weakly bound excited state, which may also be vibrationally hot (indicated by the *stack* of *horizontal lines*). Electronic relaxation and vibrational cooling take place on the same timescale.

stretch fundamental take place on the same timescale of 3–4 ps. The decay of |e⟩ may lead to the simultaneous population of both the CN $v = 1$ and $v = 0$ levels in the ligated electronic ground state. The experimental time constants can then be reproduced by setting $k_{e0} + k_{e1} \approx (3.6\ \text{ps})^{-1}$ and assuming much faster vibrational relaxation ($k_{10} > k_{e1}$). A fine tuning of the individual rates also allows one to obtain the correct signal intensities. The ''IR-invisible'' state |e⟩ in this scheme would most likely be a photolyzed state: Ligands that are able to rotate almost freely in the heme pocket may be characterized by a strongly broadened absorption band (Lim et al., 1995b; Kriegl et al., 2003). Furthermore, the large amount of energy required for the vibrational excitation of CN implies an impulsive process that can realistically only be expected as a direct result of photo excitation (C=O has been observed in the $v = 1$ state after photolysis from myoglobin, Lim et al., 1995b), but not during the decay of an electronically excited state on a 3–4-ps timescale. Thus vibrational excitation would already have to exist in state |e⟩, where it should be relatively long-lived. Upon return to the (ligated) ground state, on the other hand, vibrational excitation would have to decay rapidly (significantly faster than the lifetime of |e⟩), as would be feasible after a free-to-bound transition.

As a result, ligand dissociation and subsequent recombination on a 3–4-ps timescale would appear as a consequence of an assignment of band 2 to the $v = 1 \rightarrow v = 2$ transition of heme-bound CN^-. To critically test such an assignment, we hope to soon be able to measure the anharmonicity and vibrational relaxation time T_1 of the MbC ≡ N stretch vibration directly by infrared pump-probe spectroscopy. The proposed mechanism is only possible if the $v = 1$ lifetime of heme-bound CN^- was dramatically shortened, i.e., to ≈1 ps or less, with respect to the 30–120 ps observed in H_2O and D_2O; Hamm et al. (1997a.) A positive transient absorption signal at 385 nm has been associated with the formation of an unligated ferric heme (Ye et al., 2003), and this feature in our UV-vis data may be viewed as supporting ligand dissociation (see below). On the other hand, we also observe that the dynamics of HbICN and MbCN are almost identical. This would not be expected, if photodissociated CN^- ligands were fully exposed to the two very different heme-pocket environments. We therefore also consider an alternative interpretation of the infrared spectra, which does not rely on the formation of an ''IR-invisible'' unligated state.

Bond-weakening due to electronic excitation of heme

Although the CN molecule giving rise to band 2 may not be freely moving inside the heme pocket, its weakness (relative to the bleaching signal) and spectral position may nevertheless be due to a substantial weakening of its binding to heme. In ferrous globins the ligand stretch frequency is usually found to decrease upon binding, which is often explained by transfer of electron density from the iron d_π-orbitals (d_{xz}, d_{yz}) to the antibonding π^*-orbitals of the ligand (π-backbonding). However, back-bonding is only very weak in $Fe^{II}CN$ complexes exhibiting a C ≡ N stretch frequency that is slightly below the value for free CN^- (2058 cm^{-1} in ferrous $^{12}C^{14}N$ and 1988 cm^{-1} in ferrous $^{13}C^{15}N$ complexes of *Scapharca inaequivalvis* hemoglobin; Boffi et al., 1997). The π-interaction between ligand and heme must be even weaker in ground-state ferric CN complexes, where one expects the Fe^{III}-CN bond to be mainly due to σ-donation from the molecular orbitals of CN^- (Yoshikawa et al., 1985). Thus, transient band 2 may correspond to a C ≡ N stretch transition, which derives its spectral position and low oscillator strength from a weakening of the heme iron's ability to act as a σ-acceptor. This would be possible in an electronically excited complex with an electron configuration that strongly influences the C ≡ N bond. It has recently been argued that the (d, d) excited states of heme, characterized by a ground-state porphyrin with an excited iron d-electron configuration, may become thermally populated during the relaxation of photoexcited globins (Franzen et al., 2001). A modified d-electron configuration (for example, additional electron density in the d_z^2-orbital, which may be lowered in energy as a result of an increasing Fe-CN distance) could indeed weaken the σ-bonding interaction. If we assign band 2 to an electronically excited state, heme cooling appears to be independent of electronic excitation. Indeed, d-electron excitations of the heme iron require only relatively little energy (Gouterman, 1978), and the vibrational temperature is not expected to be very different in the ground state and a (d, d) excited state. More surprising is the observation that changes in population and shifts in the band frequencies (cooling) also take place on the same timescale (see Fig. 6 *b*). Although this could be coincidental, low frequency heme modes, that anharmonically couple to the CN-vibration, could be excited during

the decay of the electronically excited state (or ligand recombination after photodissociation), which may then become the rate-limiting step for the full thermalization of the ground-state heme.

In summary, a small red-shift of the C ≡ N stretch vibration is observed for molecules that return to the ligated electronic ground state of MbCN after Soret excitation. This is explained by anharmonic coupling of low frequency modes of the heme with excess vibrational energy, and provides a direct measure of the timescale (3–4 ps) for vibrational energy relaxation. The time evolution of this signal also reveals a quasi-instantaneous return of approximately one-quarter of the excited molecules to the ligated electronic ground state (with CN in the vibrational ground state), and a slower relaxation of the remaining species, again with a 3–4-ps time constant. The second transient absorption band, red-shifted by $\sim$30 cm^{-1} from the bleaching signal, could be assigned to heme-bound CN that has become vibrationally excited, under a mechanism which would imply ligand dissociation. Alternatively band 2 could be the signature of a more weakly bound, electronically excited state of the heme, possibly characterized by a nonequilibrium population in the iron *d*-orbitals.

Transient signals in the Soret and Q-band region

The most important observations in the UV-visible spectra are that 1), the photoinduced dynamics is independent of the specific distal protein environments of Mb and HbI and that 2), spectral features and timescales in the response of the ferric cyanide complexes are strikingly similar to results of previous measurements on globins in the ferrous state.

The transient absorption spectra of ferrous heme complexes like MbCO, MbNO, MbO_2, or the unligated deoxy form of the protein were initially interpreted in terms of two independent photocycles (Petrich et al., 1988): In one photocycle, ligand photolysis leads to the formation of the unligated deoxy species in the ground state. The unligated ground state is populated via an excited-state intermediate, often called Hb_I*. This intermediate is characterized by a short-lived (300 fs) transient absorption feature peaking at 480 nm, which is superimposed on the ground-state bleaching signal in the transient spectra at very early time delays. The ligand may then rebind to the deoxy species (geminate recombination). A second photocycle was proposed to account for the fast reformation of the ground-state ligated complexes, observed within 2–3 ps after photoexcitation for ligands like oxygen and nitric oxide. A five-coordinated intermediate state, called Hb_{II}*, with the spectral characteristics of a red-shifted Soret band, was held responsible for ultrafast rebinding in this photocycle (Petrich et al., 1988). Although this pioneering work did not evaluate the influence of vibrational energy relaxation on the transient absorption data, molecular dynamics simulations (Henry et al., 1986; Sagnella et al., 2000), time-resolved Raman (Petrich et al., 1987; Mizutani and Kitagawa, 1997, 2002), and infrared measurements (Lian et al., 1994) all point to the importance of heme-cooling after photoexcitation, which takes place on the same timescale as fast ligand dynamics ($<$10 ps), and may have a strong effect on electronic spectra in the Soret and Q-band region. Many works in the past decade have been dedicated to a clarification of these effects: by monitoring the near-infrared heme-to-iron charge transfer band III in deoxy myoglobin, Lim et al. (1996) deduced an electronic ground-state recovery in 3.4 ± 0.4 ps and an exponential cooling of heme in 6.2 ± 0.5 ps. A reinterpretation of the transient absorption data in the Soret region has recently been given in the context of absolute quantum yield measurements for ligand photodissociation of myoglobin, which was found to be 100% for MbCO, 50% for MbNO, and only 28% for MbO_2 (Ye et al., 2002). It was proposed that the molecules which remain six-coordinated immediately return to the vibrationally hot electronic ground state, characterized by a broadened and red-shifted Soret absorption band. Vibrational cooling on a femtosecond-to-picosecond timescale then accounts for the spectral dynamics previously associated with the decay of Hb_I* and Hb_{II}* (Ye et al., 2003). A careful analysis of the optical response of deoxy myoglobin in the Q-band region also led to the conclusion that vibrational cooling of heme is the main determinant for spectral evolution on the picosecond timescale (Kholodenko et al., 1999a). A somewhat different view was put forward in work by Franzen et al. (2001). Although recognizing that the Soret absorption band may strongly broaden and shift to longer wavelengths at elevated temperatures, the authors concluded that the size of the experimentally observed red-shifts could not be reproduced by considering vibrational excitation of a ground-state heme alone. Instead, Hb_{II}* was assigned to a porphyrin ground state with a thermally excited *d*-electron configuration (see above). In the same article it was postulated that the short-lived excited state Hb_I* forms independent of ligand in all ferrous heme complexes and is a signature of an iron-to-porphyrin charge transfer state. The charge transfer process, which would leave the iron in the oxidation state (III), is believed to be closely linked to the mechanism of ligand photolysis (Franzen et al., 2001).

Subpicosecond dynamics

The broad, short-lived transient absorption signal in our data on ferric MbCN strongly remind us of the spectral signature associated with Hb_I* in ferrous systems. In addition, our global analysis yields a very similar ultrafast time constant of 230 fs (compared to 250 ± 80 fs in MbCO, Franzen et al., 2001). During the first picosecond after UV excitation, there appears to be a quasi-isosbestic point at 450 nm, separating the signal decay at long wavelengths from the rise of the antibleach immediately to the red of the Soret (Fig. 1). This may support the view that this ultrafast dynamics involves

population transfer between distinct electronic states, although we note that a narrowing and shifting Soret band (due to vibrational cooling in the electronic ground state) can also produce such a spectral feature. Relaxation of the initially excited state should occur on a similar ultrafast timescale. Unfortunately, stimulated emission is not a strong observable as, for example, in chlorophylls (Visser et al., 1995), but excited state absorption from intermediate electronic states may nevertheless contribute to the broad fast-decaying signal. In a protein with a ferric heme iron, however, the assignment of an electronically excited state to an iron-to-ligand charge transfer state encounters some difficulties. The electron transferred to the porphyrin cannot originate from an iron *d*-orbital as postulated in Franzen et al. (2001), but would have to be provided from outside the heme. In this case the short timescales involved seem to limit the choice of possible electron donors to either the proximal histidine or the CN^- ligand. The proximal histidine has been considered to be involved in heme reduction (Sato et al., 1992). Transfer of an electron from the CN^- ligand to the heme may be more likely, since the Fe-CN bond in the ground state already involves partial ligand to iron charge transfer. However, full transfer of an electron would result in a CN radical with a much stronger oscillator strength for the C ≡ N stretch transition. Our mid-infrared data provides no hint to the formation of such a species, which should have been easy to detect. Thus the presence of a Hb_I*-like signal in the transient spectra of a ferric complex creates some doubt on its association with a porphyrin anion. Indeed, it has been pointed out that the 400–500-nm region is rather ill-suited for the identification of excited states in metal porphyrin complexes (Rodriguez et al., 1989), and a very detailed investigation of the near-infrared region will be necessary to clarify this point.

Picosecond dynamics

At least after delay times >0.5 ps the transient signal carries all the characteristics of a spectrally narrowing and blue-shifting product absorption band. Spectral narrowing can explain the initial increase of the positive absorption signal near 440 nm, while the increasing overlap with the ground-state bleach may contribute to its subsequent decay and cause the continuous blue-shift of the zero-crossing between Soret bleach and photoinduced absorption. The interpretation of this kind of spectral evolution in terms of vibrational energy relaxation in a hot heme was first given by Rodriguez and Holten (1989). Although vibrational cooling in that work was observed in a (*d*, *d*) excited state of four-coordinated Ni-porphyrins, it has frequently been pointed out that similar signals in ferrous heme complexes may be due to red-shifted Soret absorption of vibrationally hot molecules that are already in the electronic ground state (Lim et al., 1996; Kholodenko et al., 1999b; Cao et al., 2001; Ye et al., 2003). Here, the mid-infrared measurements help to carry out a differentiated analysis of the transient spectra in the Soret region for the ferric cyano complexes.

The time-dependent energy shift of the MbC ≡ N stretch vibration clearly shows that hot, ligated ground-state molecules are already present very early in the dynamics and that they cool down on a 3–4-ps timescale. Ultrafast electronic ground-state recovery is also indicated by the observation of the ground-state Fe-His vibrational mode of ferrous MbNO at 220 cm^{-1} without measurable phase lag in femtosecond coherence measurements (Rosca et al., 2000; Kumar et al., 2001). Cooling in the electronic ground state is consistent with a red-shifted Soret absorption band, which gradually approaches the equilibrium position. In addition, however, the two possible assignments for the small, second IR absorption band implies the existence of either an electronically excited, or a dissociated state on the same timescale.

In the case of ligand dissociation, the transient spectra in the Soret region should also reflect the formation of a five-coordinated, unligated ferric heme. The absorption spectrum of such a species, a rather broad band with a maximum at 394 nm, has recently been reported (Cao et al., 2001). We do, indeed, observe a relatively large positive signal to the blue of the ground-state Soret bleaching that decays on the required timescale and which could be attributed to an unligated heme (or a very weakly bound complex). However, similar blue-shifted transient absorption signals (although usually smaller) are observed in ferrous systems as well, and we cannot exclude that the signal in the 380-nm region is due to a strongly broadened Soret absorption of a vibrationally hot but ligated heme in the electronic ground state.

If electronic excitation is the origin of the weak transient IR band, this may or may not influence the spectra in the Soret region. Near-infrared measurements on deoxy myoglobin have identified an electronically excited state with a 1-ps lifetime and an absorption maximum at 830 nm (Lim et al., 1996). On the other hand, excited states of (*d*, *d*) character in metal porphyrins give rise to red-shifted Soret and Q-absorption bands (Rodriguez et al., 1989) due to the interaction of the nonequilibrium *d*-electron configuration with the porphyrin π-orbitals. Thus, as proposed by Franzen et al. (2001) for ferrous complexes, the transient absorption feature near 440 nm in MbCN and HbICN could, in part, be due to a distorted Soret transition. Indeed, the decay of the signal at 440 nm and of the C ≡ N stretch bleaching signal at 2126 cm^{-1}, which provides a measure for the return of molecules to the ligated electronic and vibrational (CN) ground state, take place exactly in parallel. In this context it is interesting to recall an earlier hypothesis (Waleh and Loew, 1982), which links the ultrafast relaxation of the porphyrin $\pi \rightarrow \pi^*$ excitation to the simultaneous promotion of electrons from d_π to d_z^2 or $d_{x^2-y^2}$ to d_z^2. Such a modification of the electron density in the heme iron *d*-orbitals, apart from perturbing the porphyrin absorption, may also be

responsible for the weakening of the iron ligand bond, both in ferrous and in ferric complexes.

CONCLUSIONS

Combined time-resolved UV-visible and infrared measurements of MbCN and HbICN from *L. pectinata* have been carried out and allow a detailed analysis of the photoinduced dynamics in ferric heme complexes. The UV-visible response of the cyanide complexes is independent of the specific distal protein environments despite the fact, that hemoglobin I from *L. pectinata* possesses a larger number of polar side chains than myoglobin which would be expected to alter the dynamic behavior of a charged ligand.

At very early times, the transient spectra reveal a broad absorption feature, similar to the one associated with Hb_I* in ferrous systems. This calls for a reconsideration of a recent assignment of Hb_I* to an iron-to-porphyrin CT state (Franzen et al., 2001). It can only be maintained if either the CN^- ligand or the proximal histidine are invoked as electron donors in the ferric systems.

Approximately one-quarter of the molecules return to the (hot) ligated electronic ground state already within the time resolution of the IR experiment (500 fs), as evidenced by the corresponding MbC ≡ N stretch transition. Full recovery of the ligated electronic and vibrational ground state then takes place with a 3–4-ps time constant, which dominates the decay of both IR and UV-vis spectra at longer time delays. This is very similar to the value reported for deoxy myoglobin (Lim et al., 1996), and much faster than for any other six-coordinated heme complex investigated so far. The infrared measurements allow for two alternative interpretations for the underlying mechanism. In the first case, the IR spectra would monitor the population of heme-bound ligands with and without vibrational excitation of the CN-stretch, and imply ligand dissociation with a quantum efficiency of ~75%. Complete recombination would then take place with a 3.6-ps time constant. Alternatively, the Fe-CN bond may only be weakened in an electronically excited state, possibly of (*d*, *d*)-character, leading to a downshift of the C ≡ N stretch frequency. In this case, the dominant 3.6-ps time constant corresponds to the excited-state decay. Although the dissociation hypothesis, which is based on a number of critical assumptions, cannot be ruled out completely, we prefer the latter interpretation, given the insensitivity of the transient response to the heme pocket environment.

Excited-state relaxation or, alternatively, recombination is accompanied by the vibrational cooling of a hot heme. This is evidenced by shifts of the infrared band maxima, and takes place on the same timescale as the population decay (3–4 ps). As a result, vibrational cooling and population dynamics accompany the spectral dynamics in the Soret region. Indeed, our data suggests that both processes may be linked by energy release upon electronic decay or recombination and should not be considered separately.

Given the similarity of the photodynamics of the ferric heme proteins investigated here, and observations made on ferrous globins, we believe that our findings are not specific to the ferric systems. The special property of the cyano complexes is, rather, that they provide a very sensitive local probe (in the form of the CN ligand) that allows us to monitor independently the population and cooling dynamics of a six-coordinated heme embedded in a protein.

We thank J.-L. Martin (Palaiseau) and P. M. Champion (Boston) for very valuable comments.

This research was supported in part by the American National Science Foundation Research Improvement in Minority Institutions (HRD-9550705), the National Science Foundation (MCB-9974961), and the National Institutes of Health Center for Biomedical Research Excellence (RR16439) programs (to J.L.G.), and by the Swiss National Science Foundation (via contracts 2000-067912 and 061897.00 to M.C.).

REFERENCES

Boffi, A., E. Chiancone, S. Takahashi, and D. L. Rousseau. 1997. Stereochemistry of the Fe(II)- and Fe(III)-cyanide complexes of the homodimeric *Scapharca inaequivalvis* hemoglobin. A resonance Raman and FTIR study. *Biochemistry.* 36:4505–4509.

Bredenbeck, J., and P. Hamm. 2003. Versatile small volume closed-cycle flow cell system for transient spectroscopy at high repletion rates. *Rev. Sci. Inst.* 74:3188–3189.

Cao, W., J. F. Christian, P. M. Champion, F. Fosca, and J. T. Sage. 2001. Water penetration and binding to ferric myoglobin. *Biochemistry.* 40:5728–5737.

Cerda, J., Y. Echevaria, E. Morales, and J. L. Garriga. 1999. Resonance Raman studies of the heme-ligand active site of hemoglobin I from *Lucina pectinata*. *Biospectroscopy.* 4:311–326.

Das, T. K., M. Couture, M. Guertin, and D. L. Rousseau. 2000. Distal interactions in the cyanide complex of ferric *Chlamydomonas* hemoglobin. *J. Phys. Chem. B.* 104:10750–10756.

Franzen, S., L. Kiger, C. Poyart, and J. L. Martin. 2001. Heme photolysis occurs by ultrafast excited state metal-to-ring charge-transfer. *Biophys. J.* 80:2372–2385.

Gouterman, M. 1978. Optical spectra and electronic structure of porphyrins and related rings. *In* The Porphyrins, Vol. III. D. Dolphin, editor. Academic Press, New York. 1–166.

Hamm, P., R. A. Kaindl, and J. Stenger. 2000. Noise suppression in femtosecond mid-infrared light sources. *Optics Lett.* 25:1798–1800.

Hamm, P., M. Lim, and R. M. Hochstrasser. 1997a. Vibrational energy relaxation of the cyanide ion in water. *J. Chem. Phys.* 107:10523–10531.

Hamm, P., S. M. Ohline, and W. Zinth. 1997b. Vibrational cooling after ultrafast photoisomerization of azobenzene measured by femtosecond infrared spectroscopy. *J. Chem. Phys.* 106:519–529.

Henry, E. R., W. A. Eaton, and R. M. Hochstrasser. 1986. Molecular dynamics simulations of cooling in laser-excited heme proteins. *Proc. Natl. Acad. Sci. USA.* 86:8982.

Kholodenko, Y., E. A. Gooding, Y. Dou, M. Ikeda-Saito, and R. M. Hochstrasser. 1999a. Heme protein dynamics revealed by geminate nitric oxide recombination in mutants of iron and cobalt myoglobin. *Biochemistry.* 38:5918–5924.

Kholodenko, Y., M. Volk, E. A. Gooding, and R. M. Hochstrasser. 1999b. Energy dissipation and relaxation processes in deoxy myoglobin after photoexcitation in the Soret region. *Chem. Phys.* 259:71–87.

Kraus, D. W., and J. B. Wittenberg. 1990. Hemoglobins of *Lucina pectinata* bacteria symbiosis. I. Molecular properties, kinetics and equilibria of reactions with ligands. *J. Biol. Chem.* 265:16043–16053.

Kriegl, J. M., K. Nienhaus, P. Deng, J. Fuchs, and G. U. Nienhaus. 2003. Ligand dynamics in a protein internal cavity. *Proc. Natl. Acad. Sci. USA.* 100:7069–7074.

Kumar, A. T. N., F. Rosca, A. Widom, and P. M. Champion. 2001. Investigations of amplitude and phase excitation profiles in femtosecond coherence spectroscopy. *J. Chem. Phys.* 114:701–724.

Lian, T., B. Locke, Y. Kholodenko, and R. M. Hochstrasser. 1994. Energy flow from solute to solvent probed by femtosecond IR spectroscopy: malachite green and heme protein solutions. *J. Phys. Chem.* 98:11648–11656.

Lim, M., T. A. Jackson, and P. A. Anfinrud. 1995a. Binding of CO to myoglobin from a heme pocket docking site to form nearly linear Fe-CO. *Science.* 269:962–966.

Lim, M., T. A. Jackson, and P. A. Anfinrud. 1995b. Mid-infrared vibrational spectrum of CO after photodissociation from haem: evidence for a ligand docking site in the haem pocket of haemoglobin and myoglobin. *J. Chem. Phys.* 102:4355–4366.

Lim, M., T. A. Jackson, and P. A. Anfinrud. 1996. Femtosecond near-IR absorbance study of photoexcited myoglobin: dynamics of electronic and thermal relaxation. *J. Phys. Chem.* 100:12043–12051.

Martin, J. L., and M. Vos. 1994. Femtosecond measurements of geminate recombination in heme proteins. *Meth. Enzymol.* 232:418–431.

Mizutani, Y., and T. Kitagawa. 1997. Direct observation of cooling of heme upon photodissociation of carbonmonoxy myoglobin. *Science.* 278:443–446.

Mizutani, Y., and T. Kitagawa. 2002. Vibrational energy relaxation of metalloporphyrins in a condensed phase probed by time-resolved resonance Raman spectroscopy. *Bull. Chem. Soc. Jap.* 75:623–639.

Moore, J. N., P. A. Hansen, and R. M. Hochstrasser. 1988. Iron-carbonyl bond geometries of carboxymyoglobin and carboxyhemoglobin in solution determined by picosecond time-resolved infrared spectroscopy. *Proc. Natl. Acad. Sci. USA.* 85:5062–5066.

Petrich, J. W., J. L. Martin, D. Houde, C. Poyart, and A. Orszag. 1987. Time-resolved Raman spectroscopy with subpicosecond resolution: vibrational cooling and delocalization of strain energy in photodissociated (carbonmonoxy)hemoglobin. *Biochemistry.* 26:7914–7923.

Petrich, J. W., C. Poyart, and J. L. Martin. 1988. Photophysics and reactivity of heme proteins: a femtosecond absorption study of hemoglobin, myoglobin, and protoheme. *Biochemistry.* 27:4049–4060.

Rajaratham, K., G. N. Mar, M. L. Chiu, and S. G. Sligar. 1992. Determination of the orientation of the magnetic axes of the Cyano-metMb complexes of point mutants of myoglobin by solution ^{1}H NMR: influence of His E7→ Gly and Arg CD3→ Gly substitutions. *J. Am. Chem. Soc.* 114:9048–9058.

Reddy, K. S., T. Yonetani, A. Tsuneshige, B. Chance, B. Kushkuley, S. S. Stavrov, and J. M. Vanderkooi. 1996. Infrared spectroscopy of the cyanide complex of iron(II) myoglobin and comparison with complexes of microperoxidase and hemoglobin. *Biochemistry.* 35:5562–5570.

Rizzi, M., J. B. Wittenberg, A. Coda, M. Fosano, P. Ascenzi, and M. Bolognesi. 1994. Structure of the sulfide-reactive hemoglobin from the clam *Lucina pectinata*. *J. Mol. Biol.* 244:86–99.

Rodriguez, J., and D. Holten. 1989. Ultrafast vibrational dynamics of a photoexcited metalloporphyrin. *J. Chem. Phys.* 91:3525–3531.

Rodriguez, J., C. Kirmaier, and D. Holten. 1989. Optical properties of metalloporphyrin excited states. *J. Am. Chem. Soc.* 111:6500–6506.

Rosca, F., A. T. N. Kumar, X. Ye, T. Sjodin, A. A. Demidov, and P. M. Champion. 2000. Investigations of coherent vibrational oscillations in myoglobin. *J. Phys. Chem. A.* 104:4280–4290.

Sage, J. T. 1997. Infrared crystallography: structural refinement through spectroscopy. *Appl. Spectrosc.* 51:568–573.

Sagnella, D. E., J. E. Straub, and D. Thirumalai. 2000. Time scales and pathways for kinetic energy relaxation in solvated proteins: application to carbonmonoxy myoglobin. *J. Chem. Phys.* 113:7702–7711.

Sato, S., K. Kamogawa, K. Aoyagi, and T. Kitagawa. 1992. Time-resolved resonance Raman investigation of the photoreduction of iron octaethylporphyrin complexes by using the quasi-simultaneous pump/probe measurement technique. *J. Phys. Chem.* 96:10676–10681.

Schweitzer-Stenner, R., A. Cupane, M. Leone, C. Lemke, J. Schott, and W. Dreybrodt. 2000. Anharmonic protein motions and heme deformations in myoglobin cyanide probed by absorption and resonance Raman spectroscopy. *J. Phys. Chem. B.* 104:4754–4764.

Steiger, B., J. S. Baskin, F. C. Anson, and A. H. Zewail. 2000. Femtosecond dynamics of dioxygen-picket-fence cobalt porphyrins: ultrafast release of O_2 and the nature of dative bonding. *Angew. Chem. Int. Ed.* 39:257–260.

Terwilliger, N. M. 1998. Functional adaptations of oxygen-transport proteins. *J. Exp. Biol.* 201:1085–1098.

Visser, H. M., O. J. G. Somsen, F. van Mourik, S. Lin, I. H. M. van Stokkum, and R. van Grondelle. 1995. Direct observation of subpicosecond equilibration of excitation-energy in the light-harvesting antenna of *Rhodospirillum rubrum*. *Biophys. J.* 69:1083–1099.

Vojtechovsky, J., K. Chu, J. Berendzen, R. M. Sweet, and I. Schlichting. 1999. Crystal structures of myoglobin-ligand complexes at near-atomic resolution. *Biophys. J.* 77:2153–2174.

Waleh, A., and G. H. Loew. 1982. Quantum mechanical studies of the photodissociation of carbonylheme complexes. *J. Am. Chem. Soc.* 104:2346–2351.

Wittenberg, J., and D. Kraus. 1991. Hemoglobins of Eukaryote/Procaryote Symbiotes. Springer, New York. 323–329.

Ye, X., A. Demidov, and P. M. Champion. 2002. Measurements of the photodissociation quantum yields of MbNO and MbO_2 and the vibrational relaxation of the six-coordinate heme species. *J. Am. Chem. Soc.* 124:5914–5924.

Ye, X., A. Demidov, F. Rosca, W. Wang, A. Kumar, D. Ionascu, L. Zhu, D. Barrick, D. Wharton, and P. M. Champion. 2003. Investigations of heme protein absorption line shapes, vibrational relaxation, and resonance Raman scattering on ultrafast time scales. *J. Phys. Chem. A.* 107:8156–8165.

Yoshikawa, S., D. H. O'Keeffe, and W. S. Caughey. 1985. Investigations of cyanide as an infrared probe of hemoprotein ligand binding sites. *J. Biol. Chem.* 260:3518–3528.